TÜBİTAK

Turkish Journal of Veterinary and Animal Sciences

http://journals.tubitak.gov.tr/veterinary/

Research Article

Turk J Vet Anim Sci
(2019) 43: 834-845

doi:10.3906/vet-1810-61

Phenotypic characterization and differentiation of mesenchymal stem cells originating from adipose tissue

Ece ÇERÇİ, Hatice ERDOST*

Department of Histology and Embryology, Faculty of Veterinary Medicine, Uludağ University, Görükle, Bursa, Turkey

Received: 23.10.2018 • **Accepted/Published Online:** 26.09.2019 • **Final Version:** 03.12.2019

Abstract: Stem cells are known as undifferentiated cells that are capable of divisions and self-renewal over an extended period. Adipose tissue-derived mesenchymal stem cells (ADSCs) are known to differentiate into many different organ and tissue cells. The purpose of this study was to characterize adipose tissue-derived mesenchymal stem cells in detail based on the expression status of certain surface markers and differentiation stages for clinical and laboratory applications. The migrating phase and mitotic property of the cells from adipose tissue were assessed under a microscope. Cell counting was performed during the first, second, and third passages. The cells were differentiated into osteogenic, chondrogenic, and adipogenic lineages. Stem cells were characterized by immunostaining of CD90, CD105, CD11b, and CD45 surface markers. ADSC growth kinetics were determined at the first, second, and third passages. In conclusion, ADSCs were reported in detail here based on surface markers and differentiation potentials, growth curves, and population doubling times during the first, second, and third passages.

Key words: ADSCs, differentiation, characterization, growth curve, population doubling time

1. Introduction

Isolation techniques for adipose cells from rat tissue were pioneered by Rodbell in the 1960s [1]. Mesenchymal stem cells (MSCs) can be isolated from mammalian animal tissues such as tendon, synovial membrane, bone marrow, liver, dental pulp, adipose tissue, placenta, amniotic fluid, and amniotic cord blood [2]. The isolation procedure for stem cells from adipose tissue is relatively less invasive compared to that for bone marrow-derived mesenchymal stem cells (BMSCs) [3]. The International Society of Cellular Therapy (ISCT) defined that MSCs must be able to be differentiated into at least three lineages (osteoblast, chondroblast, and adipocyte cells). Also, they must have the capacity to attach to plastic surfaces for in vitro cultivation [4].

MSCs are characterized by the presence or absence of certain surface markers [4]. Adipose-derived stem cells (ADSCs) are characterized by the expression of certain stem cell surface markers such as CD105, CD90, CD73, and CD44 and the lack of CD45, CD34, CD14, and CD11b expression. ADSCs have some advantages over other multipotent stem cell types, including accessibility to fat tissue and faster proliferation capability [5,6].

The purpose of this study is to describe the details of the steps for isolation of mesenchymal stem cells, characterization with surface markers, differentiation potentials, growth curves, and population doubling times during the first, second, and third passages for tissue engineering and regenerative medicine, especially in cases of limited starting material.

2. Materials and methods

2.1. Animals

Ethical approval was received from the Uludağ University Local Ethics Committee of Animal Experiments (2015-07/01). Four Sprague Dawley rats of 3 months old were used for fat tissue collection.

2.2. Isolation and culturing of ADSCs

Prior to initiating this experimental protocol, rats' fur was wetted with 70% ethanol (Cat. No: 65350-M; Merck, Germany). After the tissue sample transferring phase from the normal laboratory to a cell culture laboratory, tissue samples were immediately rinsed with sterile D-PBS 10 times in a separate sterile plastic cell culture plate (Millipore, Germany; Cat. No: BSS-1006). Approximately 1.5 g of adipose tissue per rat was collected from the abdominal and subcutaneous fat under sterile conditions. The nonenzymatic culture method was used for the isolation of ADSCs [6].

* Correspondence: edost@uludag.edu.tr

Adipose tissue fragments were then minced in thicknesses of 3–4 mm and transferred to rat MSC-specific growth medium (Cyagen, USA; Cat. No: RAXMD-03011-440). Growth medium contained 100 units/mL penicillin, 100 µg/mL streptomycin (GIBCO, Ireland; Cat. No: TMS-AB2-C), 2 mM L-glutamine (GIBCO; Cat. No: G7513), and 20% heat-inactivated fetal bovine serum (GIBCO; Cat. No: TMS-013-B). Tissue fragments were incubated in tissue culture flasks of 25 cm^2 under standard culture conditions (5% CO_2, in a humidified air atmosphere of 96%, at 37 °C). The culture medium was replaced with fresh medium once every three days to avoid possible differentiative effects of various cytokines originating from the MSCs and to restore nutrient depletion.

2.3. Cell counting and population doubling time

Trypan blue staining was performed to analyze the cell viability at passage 1 (P1), passage 2 (P2), and passage 3 (P3). For counting, a 1:1 ratio was used (100 µL cell suspension with 100 µL of trypan blue). Cell solution (10 µL) was added to Thoma slides during the subculturing periods of P1, P2, and P3.

Population doubling time (PDT) is defined as the time in which the number of cells doubles in a culture. Viable cells were counted using an inverted microscope to determine growth kinetics and cells were seeded per 35-mm^2 cell culture plate.

The population doubling number (PDN) and PDT were calculated using the following equations:

$PDT = CT / PDN,$

$PDN = \log (N/ N_0) \times 3.31,$

where CT is time of cultivation between days, N is cell number at the end of the cultivation period, and N_0 is cell number at culture initiation [5]. In the second equation, N and N_0 are numbers of cells at the end and beginning of the culture period, respectively. In this study the culture period of P1, P2, and P3 counted to determine proliferation potential for determining PDT was seven days.

2.4. Multilineage differentiation of adipose-derived stem cells

2.4.1. Osteogenic differentiation

ADSCs (6×10^4 cells/cm^2) were seeded in 24-well culture plates. MSCgo Osteogenic Differentiation Medium (Biological Industries, Israel; Cat. No: 05-440-1B) was added when cells reached 80% confluency. The P3 cell osteogenic differentiation medium was replaced with a fresh portion. The medium was then replaced every 2–3 days. The cultures were examined and photographed under an inverted microscope (Nikon-Eclipse). After 21 days, cells were stained with Alizarin red [7].

2.4.2. Chondrogenic differentiation

ADSCs (1×10^6 cells/cm^2) were seeded in 96-well culture plates. MSCgo Chondrogenic Differentiation Basal Medium (Biological Industries; Cat. Nos: 05-220-1B and 05-221-1D) was added when cells reached 80% confluency. The P3 chondrogenic differentiation medium was replaced with a fresh portion. The medium was then replaced every 2–3 days. The cultures were examined and photographed under an inverted microscope (Nikon-Eclipse). Cells were incubated in the chondrogenic medium for 21 days and stained with Alcian blue [7].

2.4.3. Adipogenic differentiation

ADSCs (6×10^4 cells/cm^2) were seeded in 24-well plates. The standard medium was replaced with MSCgo Adipogenic Differentiation Basal Medium (Biological Industries; Cat. Nos: 05-330-1B, 05-331-1-01, and 05-332-1-15) when cells reached 80% confluency. The P3 cell culture medium was replaced with a fresh portion. The medium was then replaced every 2–3 days. The cultures were examined and photographed under an inverted microscope (Nikon-Eclipse). After two weeks the cells were stained with Oil red O [7]

2.5. Characterization of ADSCs by immunohistochemistry

P3 ADSCs were detached using trypsin/EDTA 0.02% (PAN-Biotech, Germany; Cat. No: P10-019100) and were counted. Forty thousand ADSCs (cells/cm^2) were seeded on 8-well plastic culture slides for immunostaining and transferred to a CO_2 incubator for cell adhesion (standard conditions: 5% CO_2, 37 °C, 96% humidity) for 24 h. The cells were fixed with 4% paraformaldehyde (Merck; Cat. No: 1.04005.1000) for 1 h at room temperature and then with methanol for 15 min at –20 °C. Cells were rinsed with phosphate-buffered saline (PBS) (Sigma, USA; Cat. No: P4417-100TAB) four times. Cells were permeabilized with Triton-X 100 (Sigma; Cat. No: T8787) for 10 min and rinsed with PBS. Afterwards, these cells were incubated for 10 min with 3% hydrogen peroxidase and then rinsed with PBS. A blocking step was performed for 5 min at room temperature. The cells were incubated with CD90 (1:700 dilution; Abcam, UK; Cat. No: ab225), CD105 (1:100 dilution; Abcam; Cat. No: ab156756), CD45 (1:200 dilution; Abcam; Cat. No: ab8879), and CD11b (1:200 dilution; Abcam; Cat. No: ab10558) stem cell surface primary antibodies for 18 h at 4 °C in a humidity chamber. The cells were then incubated with secondary antibody (Thermo Scientific, USA; Cat. No: TP-125-HL) for 10 min and streptavidin-peroxidase solution was added for 10 min. Finally, the bound antibody complexes were stained with chromogen solutions for 3–5 min and then counterstained with hematoxylin.

2.6. Statistical analyses

For growth curves and population doubling times, cell numbers were expressed as mean ± SE. Cell viability was analyzed using t-tests and PDN and PDT analyzed using

ANOVA. All statistical analyses were carried out using SPSS 23.

3. Results

ADSCs at P1 exhibited a migration phase from adipose tissue in the isolation phase (Figures 1A and 1B), P1 exhibited a fibroblast-like morphology under the microscope (Figures 1C and 1D), and ADSCs at P2 exhibited confluency (Figures 1E and 1F). ADSCs at P3 exhibited a flattened, fibroblast-like morphology with regular cytoplasm and increased proliferation potential (Figure 1G) compared to P1 and P2. Cells at P3 appeared to consist of a more homogeneous population than the cells at P1 and P2 (Figure 1H). Cell numbers of ADSCs isolated from 1.5 g of adipose tissue were 8×10^6, 30×10^6, and 22×10^6 at P1, P2, and P3, respectively (Table 1).

In P1, after cell confluency in four T25 flasks, 8×10^6 cells/cm^2 were obtained (cell density: 2.1×10^6 cells/cm^2, 2.2×10^6 cells/cm^2, 1.8×10^6 cells/cm^2, and 1.9×10^6 cells/cm^2).

In P2, after cell confluency in two T25 flasks and three T75 flasks, 30×10^6 cells/cm^2 were obtained (cell density: 2.5×10^6 cells/cm^2, 2.5×10^6 cells/cm^2, 8.3×10^6 cells/cm^2, 8.4×10^6 cells/cm^2, and 8.3×10^6 cells/cm^2).

In P3, after cell confluency in one T25 flask and three T75 flasks, 22×10^6 cells/cm^2 were obtained (cell density: 2×10^6 cells/cm^2, 6.7×10^6 cells/cm^2, 6.5×10^6 cells/cm^2, and 6.8×10^6 cells/cm^2).

In this study, the osteoblastic morphology of ADSCs at P3 was first noticed on the 14th day (Figures 2A and 2B). Development of mineralized extracellular and cellular matrix nodules in these cells continued from day 5 until day 21 (Figure 2C). Osteoblasts were detected using Alizarin red staining on day 21 (Figure 2D).

The chondrogenic morphology of ADSCs at P3 was noticeable starting on day 14 in the present study (Figures 3A and 3B). The Alcian blue staining confirmed the presence of proteoglycans, suggesting the formation of cartilage matrix on day 21 (Figures 3C and 3D).

The differentiation of ADSCs at P3 into adipocytes was confirmed by the presence of prominent lipid droplets. The cells undergoing adipogenic differentiation started to exhibit a vacuolar morphology on day 5. Fat cells were detected by Oil red O staining on day 14 (Figures 4A–4D). ADSCs were negative for hematopoietic markers CD11b and CD45 (Figures 5A–5D), while they were positive for mesenchymal surface markers CD90 and CD105 (Figures 6A–6D) as assessed by immunohistochemical analyses.

Growth curve analyses were performed for seven consecutive days for P1, P2, and P3 cells. The mean values of viable cells at P1, P2, and P3 were 591 ± 22.01, 646.42 ± 57.96, and 723.57 ± 42.5, respectively (Table 2). In the subculture period, while there were no significant differences in cell numbers between P1 and P2, there were higher numbers of cells at P3 than P1 ($P < 0.05$) (Table 2; Figure 7A). However, P2 cells exhibited a faster growth pattern compared to P1 and P3 cells based on logarithmic growth curve analysis ($P < 0.05$) (Figure 7B). The P2 cells had faster proliferation capacity compared to P1 and achieved faster confluence. The cell population doubling number (PDN) was calculated for all three passages. The PDN was significantly lower for P2 cells as compared to P1 and P3 cells ($P < 0.001$) (Table 3; Figure 7C). Accordingly, P2 cells displayed a higher PDT as compared to P1 and P3 cells ($P < 0.01$) (Table 4; Figure 7D).

4. Discussion

MSCs are not subjected to the same constraints as embryonic stem cells and ADSCs can be noninvasively obtained from adipose tissue [6–8]. MSCs have a large number of cell sources and they are known as a suitable population for the use of clinical or research studies in human and animal science [9–15]. Nancy et al. [6] showed that nonenzymatic isolation results in a substantially higher yield of ADSCs at isolation phase per gram of initial adipose tissue. In the present study, ADSCs that were isolated using the nonenzymatic method exhibited faster proliferative and migration properties (P1). Bonab et al. [12] showed that the first, second, and third passages of cells derived from bone marrow lasted for 15, 10, and 12 days, respectively. Our study showed that the first, second, and third passages of cells derived from adipose tissue lasted for 8, 13, and 18 days, respectively. Niyaz et al. [16] used a nonenzymatic technique and three male Wistar albino rats for cell isolation but there were no data shown for the rats' ages. Their results showed that after 7 days only fibroblast-like cells were detected and complete confluence was not exhibited in 6-well cell culture plates. In the present study we used 3-month-old male Sprague Dawley rats and T25 flasks for isolation of cells. First complete confluence was shown on day 8. Niyaz et al. [16] noted the isolation of primary cells similarly to our results in accordance with complete cell confluence time. On day 8, we obtained complete confluency, which may be related to types of cell culture plates, genotypes of rats, ages of rats, and cell culture and laboratory techniques.

Özen et al. [17] showed that ADSCs obtained by the nonenzymatic method had higher affinity to plastic surfaces and exhibited faster proliferative capacity, as well as accelerated disappearance of erythrocytes from culture. Our results were similar to those of Özen et al. [17] regarding the proliferative potential and homogeneity of the cell population. Lendeckel et al. [18] noted that ADSCs have more proliferative capacity than BMSCs, particularly those from pediatric patients: 295 million mononuclear cells were expanded from 42.3 g of adipose tissue and

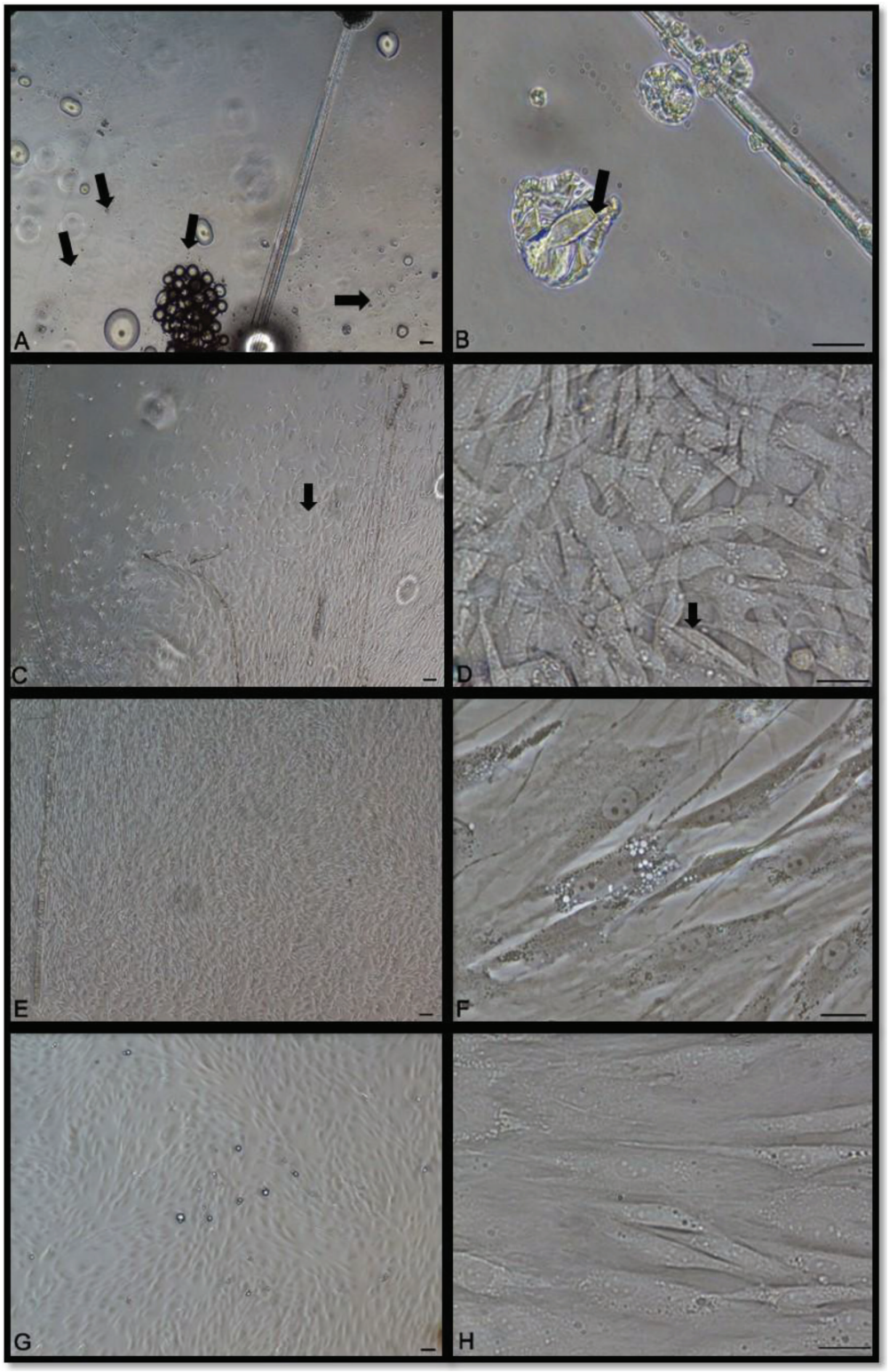

Figure 1. A) ADSCs started to exhibit migration phase from adipose tissue in isolation phase (arrows) (bar: 100 µm). B) Fibroblast-like cell (arrow) (bar: 25 µm). C) Primary passage confluency (arrow) (bar: 100 µm). D) ADSCs exhibited fibroblast-like cell morphology at P1 (arrow) (bar: 25 µm). E) ADSCs started to reach confluence at P2 (bar: 100 µm). F) ADSCs at P2 exhibited confluency (bar: 25 µm). G) ADSCs at P3 exhibited a flattened, fibroblast-like morphology with regular cytoplasm (arrows) (bar: 100 µm). H) Cells at P3 appeared to consist of a more homogeneous cell population (bar: 25 µm).

Table 1. Cell numbers in P1, P2, and P3 from 1.5 g of adipose tissue-derived mesenchymal stem cells.

	T25 culture flask	T75 culture flask	Total cell number
P1 cell number	4	-	8×10^6
P2 cell number	2	3	30×10^6
P3 cell number	1	3	22×10^6

approximately 2%–3% of these cells were assumed to be stem cells in enzymatic isolation. In our study 22 million cells in P3 were isolated from 1.5 g of adipose tissue.

In the work of Halvorsen et al. [19], stromal cells were trypsinized and plated in multiple-well plates at 3×10^4 cells/cm^2, but we used 6×10^4 cells/cm^2 to allow for attachment in stromal media. We found that, during osteogenic differentiation, the fibroblast-like phenotype of P3 cells was first noticed on day 14 and differentiation into osteoblastic

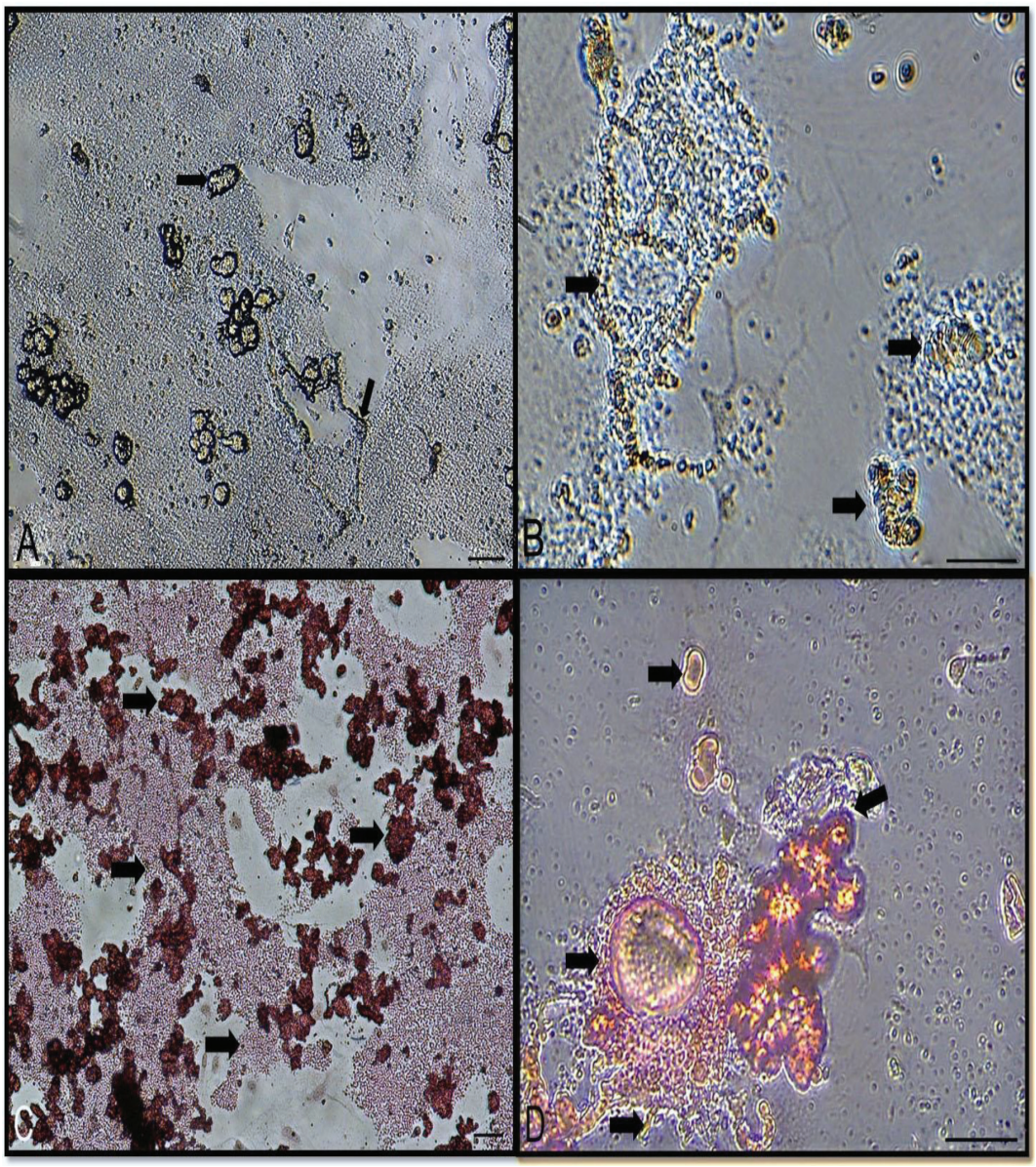

Figure 2. A, B) P3 ADSCs started to exhibit osteoblastic morphology on day 14 (thin arrows). C, D) Extracellular calcium deposition and osteoblastic morphology as demonstrated by positive Alizarin red S staining on day 21 (thick arrow) (bar: 25 μm).

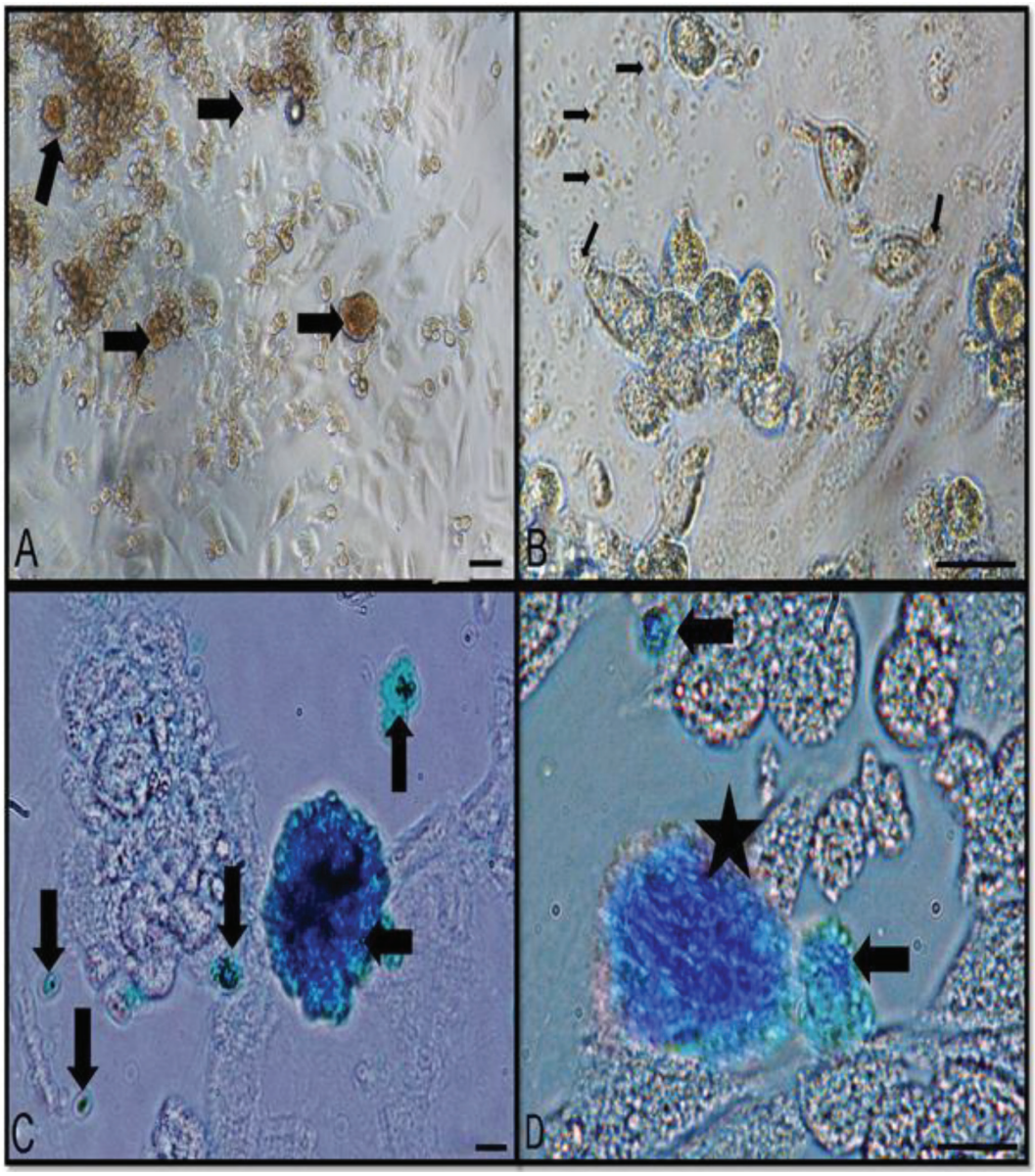

Figure 3. A, B) P3 ADSCs started to exhibit chondroblastic morphology and accumulate proteoglycan aggregates on day 14 (arrows). C, D) Staining of chondroblast precursor cell by alcian blue (arrows and *) (bar: 25 µm).

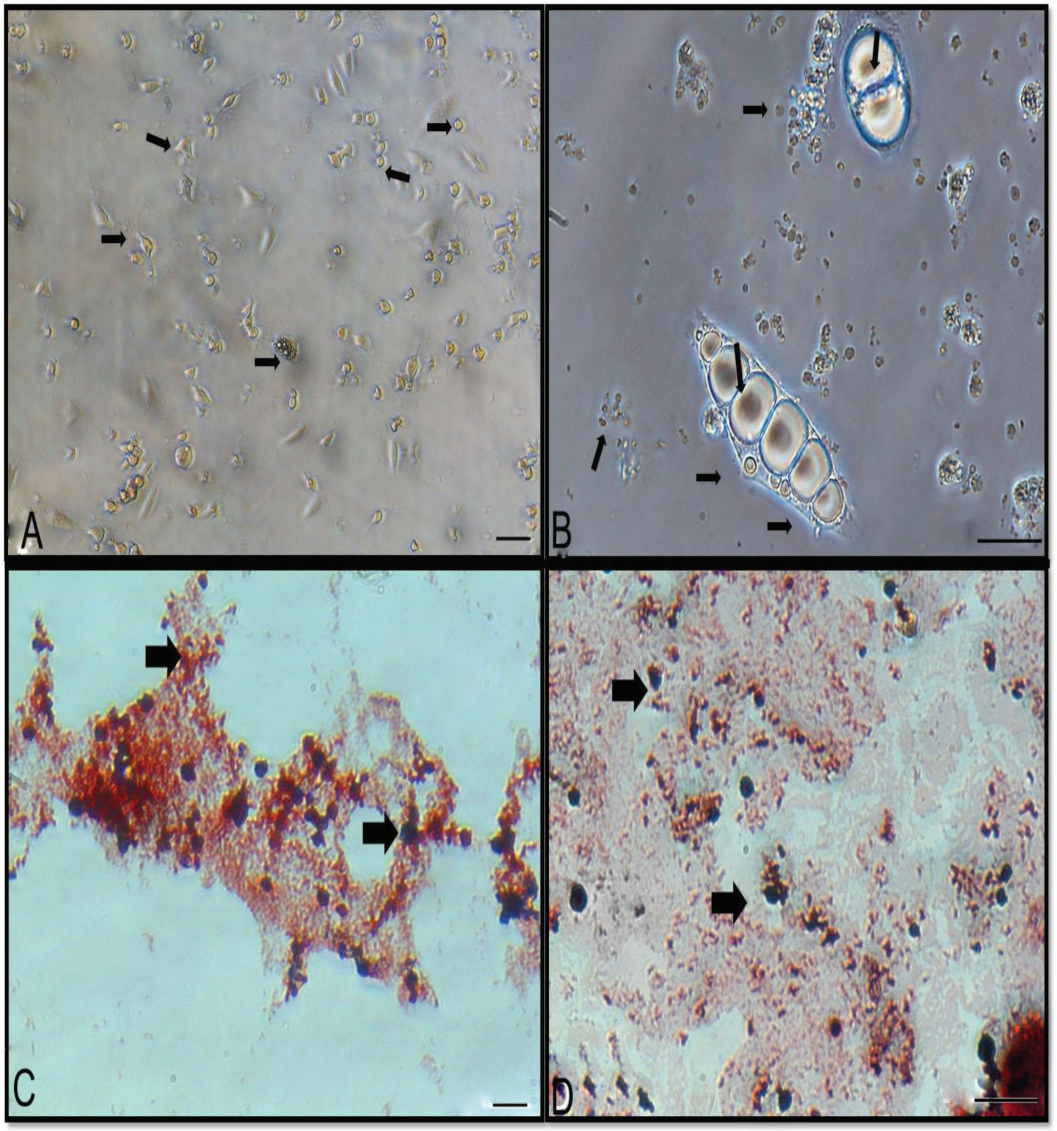

Figure 4. A, B) P3 ADSCs started to exhibit adipocyte cell morphology (arrows) with lipid droplets on day 6 (arrows). C, D) Vacuolar cell membrane of adipocytes (arrows) stained with Oil red O on day 14 (bar: 25 µm).

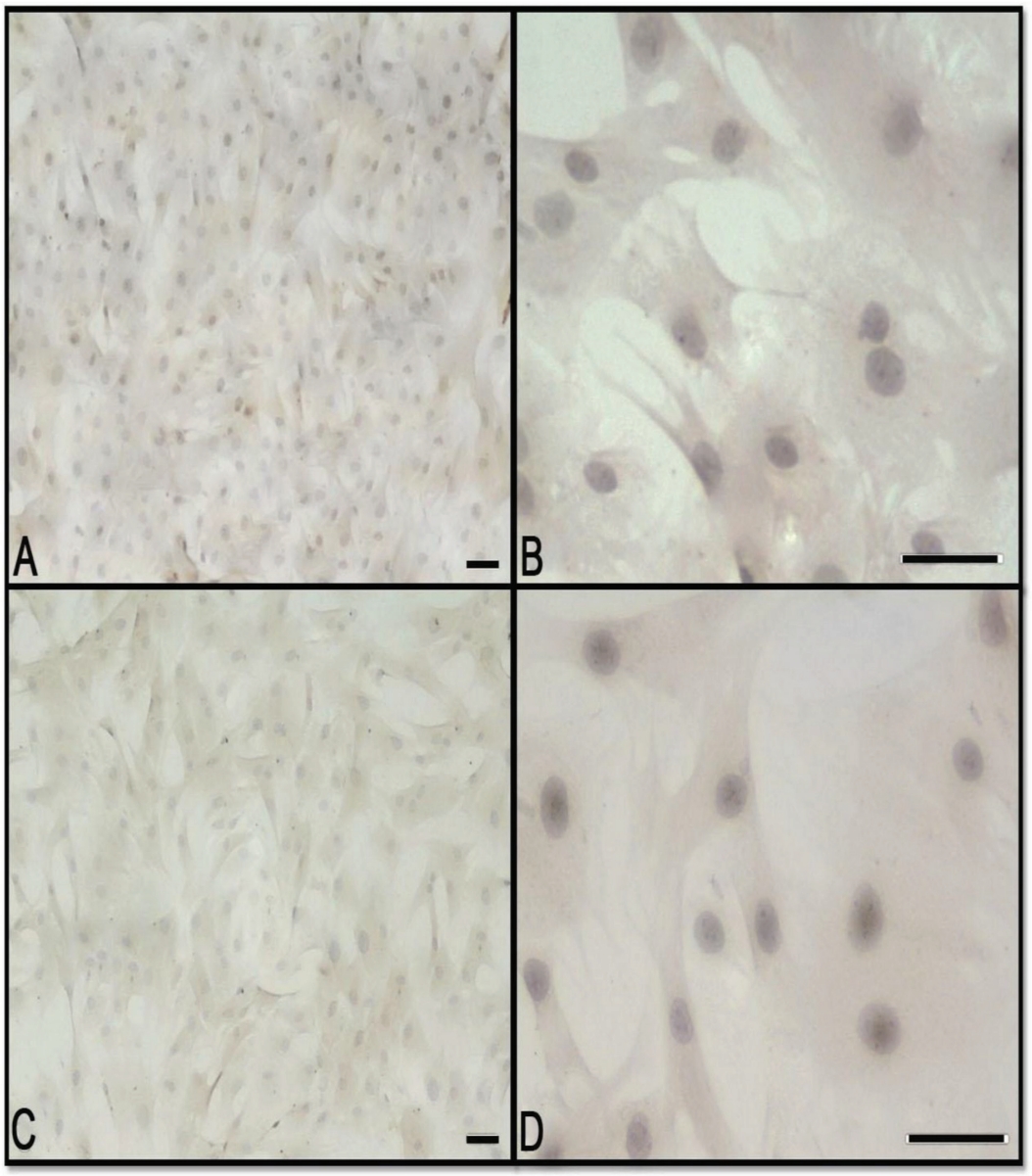

Figure 5. P3 ADSCs did not express CD11b (A, B) or CD45 (C, D) surface markers, as assessed by immunohistochemistry (bar: 25 μm).

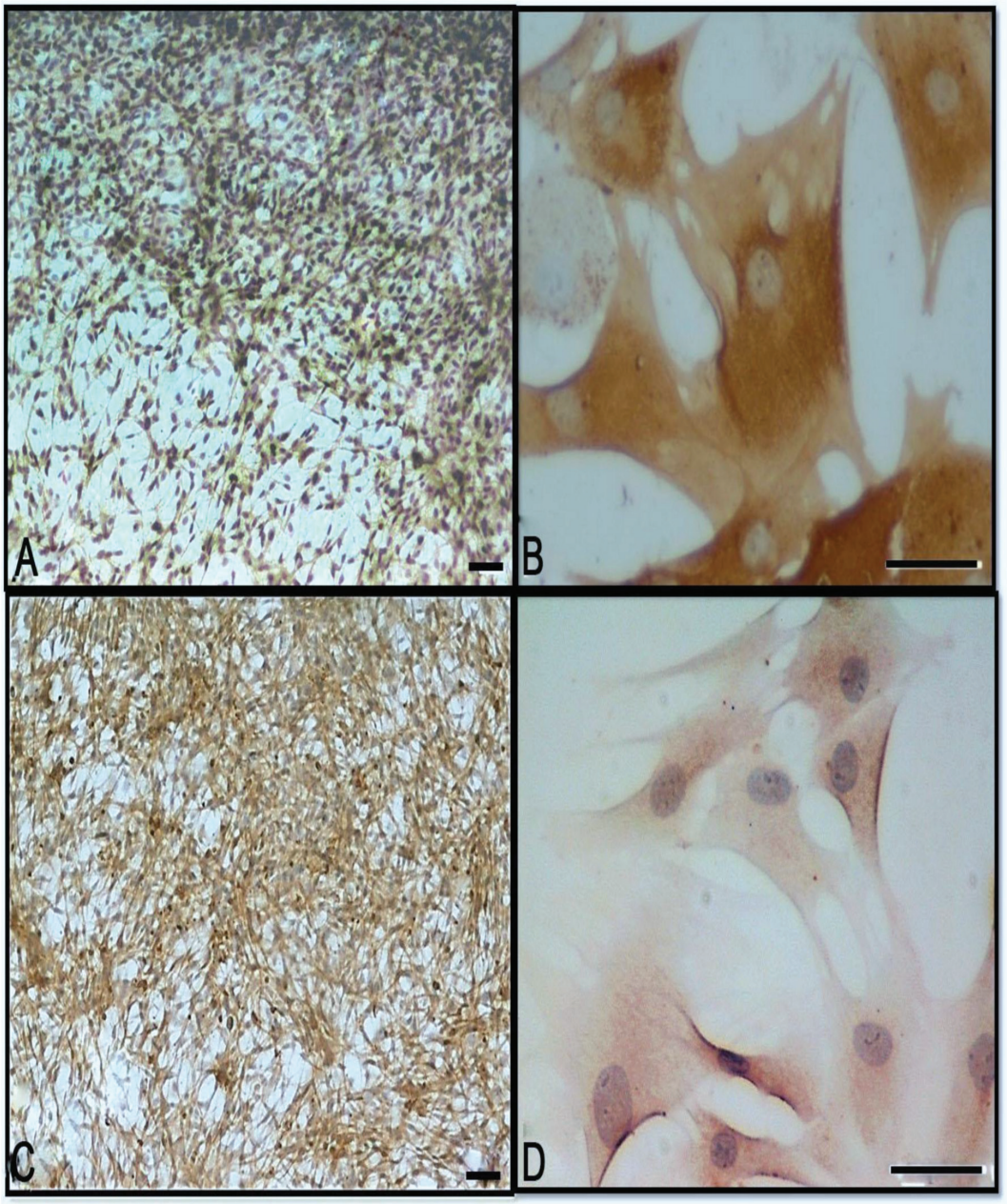

Figure 6. P3 ADSCs expressed CD90 (A, B) and CD105 (C, D) surface markers, as assessed by immunohistochemistry (bar: 25 μm).

Table 2. Cell counts and mean values of P1, P2, and P3 cells throughout seven days (total cell count: $\times 10^4$ cells/mL).

P1 viable cells		P2 viable cells	P3 viable cells
1st day	520,000	425,000	900,000
2nd day	540,000	450,000	800,000
3rd day	615,000	630,000	800,000
4th day	625,000	700,000	690,000
5th day	687,000	750,000	660,000
6th day	600,000	760,000	585,000
7th day	550,000	810,000	630,000
Mean values	591 ± 22.01[a]	646.42 ± 57.96	723.57 ± 42.5[b]

[a, b] indicate statistically significant differences for values on the same line, $P < 0.05$.

cells was completed in 21 days. Activation of stem cells is critical in the generation of osteocytes. In this study, a specific osteogenic differentiation medium was used. Halvorsen et al. [19] demonstrated an increase in osteocalcin secretion during the osteogenic differentiation phase from day 3 until day 18. Microscopically, we observed the accumulation of mineralized matrix nodules starting on day 7, which continued to increase until day 21. Mineralized matrix nodule appearance and Alizarin red staining indicated an osteoblast pattern resembling that observed by Halvorsen et al. [19].

In a study conducted by Yoshimura et al. [20], 8×10^5 cells were cultured and differentiated into chondroblasts using a pellet culture system in 21 days, while in our study, in accordance with that of Kim et al. [21], 1×10^6 ADSCs cells were seeded for the chondrogenic differentiation phase.

In most studies [15–19,22,23], the differentiation of ADSCs into adipocytes was completed in a maximum of 14 days. In that of Halvorsen et al. [19], 3×10^4 cells/cm^2 were cultured and differentiated into adipocytes, but we used 6×10^4 cells/cm^2 for adipogenic differentiation, as did Baker et al. [24]. Subsequently, ADSCs were differentiated into adipocyte precursor cells, confirmed by the presence of prominent neutral lipid droplets. ADSCs started to develop vacuolar cellular formations within 5 days and full differentiation was completed in 14 days.

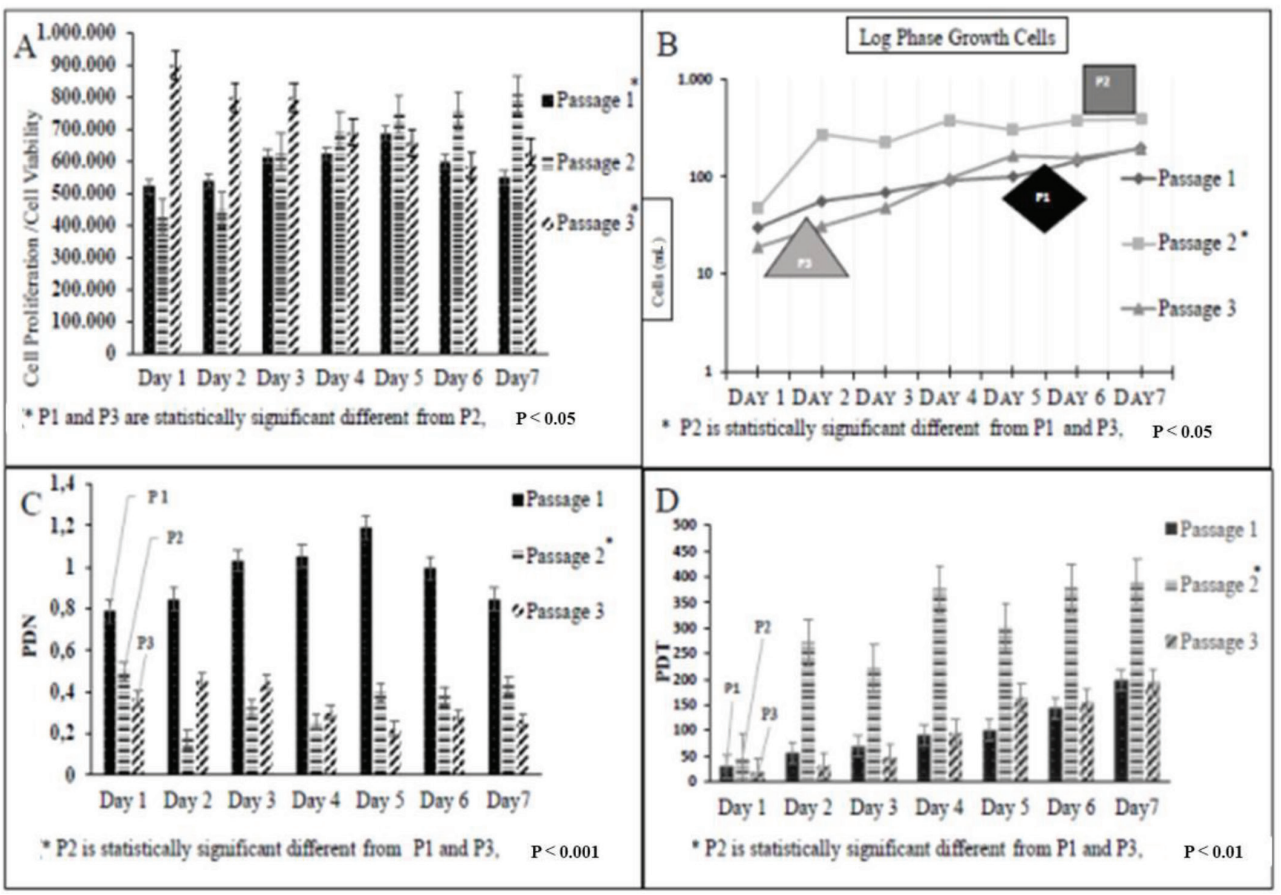

Figure 7. A) Total cell count of P1, P2, and P3 cells. B) Growth curve analyses of P1, P2, and P3 cells. C) Population doubling number (PDN) analyses of P1, P2, and P3 cells. D) Population doubling time (PDT) analyses of P1, P2, and P3 cells.

Table 3. The cell population doubling number values in P1, P2, and P3 cells throughout seven days. PDN value: $\log_{10}$ (q). Total cells were counted within 1 mL; PDT and PDN calculated for intervals of 24, 48, 72, 96, 120, 144, and 168 h.

	P1 PDN values	P2 PDN values	P3 PDN values
1st day	0.790423243	0.500019369	1,215948099
2nd day	0.844951992	0.176091259	1.51057157
3rd day	1.03190528	0.322219295	1.480093084
4th day	1.052789639	0.255272505	0.996409286
5th day	1.191055447	0.397940009	0.728557771
6th day	0.996409286	0.380211242	0.922674419
7 th day	0.844951992	0.431363764	0.868713107
Mean values	0.965 ± 0.0542[a]	0.352 ± 0.0415[b]	1.103 ± 0.115[a]

[a, b] indicate statistically significant differences for values on the same line, $P < 0.001$.

Table 4. Cell population doubling time (PDT) values in P1, P2, and P3 cells throughout seven days.

	P1 PDT values	P2 PDT values	P3 PDT values
1st day	30	47	19
2nd day	56	272	31
3rd day	69	223	48
4th day	91	376	96
5th day	100	301	164
6th day	144	378	156
7 th day	198	389	193
Mean values	98.28 ± 21.49[a]	284.42 ± 45.91[b]	101 ± 26.68 [a]

[a, b] indicate statistically significant differences for values on the same line, $P < 0.01$.

ADSC characterization has been reported in many studies and by the ISCT [3,4,16,17,22]. ADSC populations have been shown to express ≥95% CD73, CD90, and CD105 and to lack hematopoietic markers CD45 and CD11b [10,16,19,25–29]. In accordance with the published data, ADSCs in this study were positive for CD90 and CD105 and negative for CD45 and CD11b surface markers as assessed by immunohistochemistry. In our study, we showed that expression patterns of cell surface markers on P3 cells were associated with MSCs [28–30]. El Atat et al. [31] reported that ADSCs displaying CD90 and CD105 expressions were able to adhere to plastic surfaces under in vitro culture conditions. Moreover, these markers have also been used to determine multilineage differentiation capabilities of ADSCs [30]. The minimum homogeneity of MSCs was observed as 98.68% positive for CD29, CD90, CD54, and MHC Class I by flow cytometry analysis [16]. In our study, we used CD90 and CD105 positive markers, and CD90 was strongly positive compared to CD105 immunohistochemically. Similar results were shown by Niyaz et al. [16].

Our study revealed that about 22 million ADSCs of P3 were isolated from 1.5 g of adipose tissue. This is necessary for tissue engineering and regenerative medicine, especially in cases of limited starting material. In conclusion, ADSCs' isolation, characterization, differentiation, growth curves, and population doubling times were reported here in detail to contribute to the literature knowledge.

Acknowledgment
The Scientific Research Projects Coordination Unit of Uludağ University supported the present study (OUAP 2015/25).

References

1. Rodbell M. Metabolism of isolated fat cells. Journal of Biological Chemistry 1967; 242: 5751-5756.
2. Liu L, Cheung TH, Charville GW, Rando TA. Isolation of skeletal muscle stem cells by fluorescence-activated cell sorting. Nature Protocols 2015; 10: 1612-1624.
3. Hayashi O, Katsube Y, Hirose M, Ohgushi H, Ito H. Comparison of osteogenic ability of rat mesenchymal stem cells from bone marrow, periosteum, and adipose tissue. Calcified Tissue International 2008; 82: 238-247.
4. Dominici M, Le Blanc K, Mueller I, Slaper-Cortenbach I, Marini F et al. Minimal criteria for defining multipotent mesenchymal stromal cells. Cytotherapy 2006; 8: 315-317.
5. Miguélez-Rivera L, Pérez-Castrillo S, González-Fernández ML, Prieto-Fernández JG, López-González ME et al. Immunomodulation of mesenchymal stem cells in discogenic pain. North American Spine Society 2018, 2: 330-342.
6. Nancy P, Shilpita S, Sen M, Swathi S. Explant culture: a simple, reproducible, efficient and economic technique for isolation of mesenchymal stromal cells from human adipose tissue and lipoaspirate. Journal of Tissue Engineering and Regenerative Medicine 2012; 4: 524-531.
7. Braun J, Hack A, Weis-Klemm M, Conrad S, Treml S et al. Evaluation of the osteogenic and chondrogenic differentiation capacities of equine adipose tissue-derived mesenchymal stem cells. American Journal of Veterinary Research 2010; 71: 1228-1236.
8. Mizuno H, Tobita M, Uysal AC. Concise review: adipose-derived stem cells as a novel tool for future regenerative medicine. Stem Cells 2013; 30: 804-810.
9. Szöke K, Daňková J, Buzgo M, Amler E, Brinchmann JE et al. The effect of medium composition on deposition of collagen type 1 and expression of osteogenic genes in mesenchymal stem cells derived from human adipose tissue and bone marrow. Process Biochemistry 2017; 59: 321-328.
10. Tajima S, Tobita M, Mizuno H. Bone regeneration with a combination of adipose-derived stem cells and platelet-rich plasma. Methods in Molecular Biology 2018; 97331: 372-387.
11. Tropel P, Noël D, Platet N, Legrand P, Benabid AL et al. Isolation and characterisation of mesenchymal stem cells from adult mouse bone marrow. Experimental Cell Research 2004; 295: 395-406.
12. Bonab MM, Alimoghaddam K, Talebian F, Ghaffari SH, Ghavamzadeh A et al. Aging of mesenchymal stem cell in vitro. BMC Molecular and Cell Biology 2006; 7: 14.
13. Kobolak J, Dinnyes A, Memic A, Khademhosseini A, Mobasheri A. Mesenchymal stem cells: identification, phenotypic characterization, biological properties and potential for regenerative medicine through biomaterial microengineering of their niche. Methods 2016; 99: 62-68.
14. Chen JY, Mou XZ, Du XC, Xiang C. Comparative analysis of biological characteristics of adult mesenchymal stem cells with different tissue origins. Asian Pacific Journal of Tropical Medicine 2015; 8: 739-746.
15. Zuk P, Zhu M, Ashjian P, Ugarte D, Huang J et al. Human adipose tissue is a source of multipotent stem cells. Molecular Biology of the Cell 2002; 13: 4279-4295.
16. Niyaz M, Gürpınar ÖA, Günaydın S, Onur MA. Isolation, culturing and characterization of rat adipose tissue derived mesenchymal stem cells: a simple technique. Turkish Journal of Biology 2012; 36: 658-664.
17. Özen A, Gül Sancak İ, Ceylan A, Özgenç Ö. Isolation of adipose tissue derived stem cells. Turkish Journal of Veterinary and Animal Sciences 2016; 40: 137-141.
18. Lendeckel S, Jödicke A, Christophis P, Heidinger K, Wolff J et al. Autologous stem cells (adipose) and fibrin glue used to treat widespread traumatic calvarial defects: case report. Journal of Cranio-Maxillofacial Surgery 2004; 32 (6): 370-373.
19. Halvorsen YDC, Franklin D, Bond AL, Hitt DC, Auchter C et al. Extracellular matrix mineralization and osteoblast gene expression by human adipose tissue-derived stromal cells. Tissue Engineering 2001; 7: 729-741.
20. Yoshimura K, Shigeura T, Matsumoto D, Sato T, Takaki Y et al. Characterization of freshly isolated and cultured cells derived from the fatty and fluid portions of liposuction aspirates. Journal of Cellular Physiology 2006; 208: 64-76.
21. Kim DS, Lee MW, Ko YJ, Chun YH, Kim HJ et al. Cell culture density affects the proliferation activity of human adipose tissue stem cells. Cell Biochemistry & Function 2016; 34: 16-24.
22. Zuk P, Zhu M, Mizuno H, Huang J, Futrell J et al. Multilineage cells from human adipose tissue: implications for cell-based therapies. Tissue Engineering 2001; 7: 211-228.
23. Takemitsu H, Zhao D, Yamamoto I, Harada Y, Michishita M et al. Comparison of bone marrow and adipose tissue-derived canine mesenchymal stem cells. BMC Veterinary Research 2012; 8: 150.
24. Baker NA, Muir LA, Lumeng CN, O'Rourke RW. Differentiation and metabolic interrogation of human adipocytes. Methods in Molecular Biology 2017; 1566: 61-76.
25. Baghaei K, Hashemi SM, Tokhanbigli S, Rad AA, Assadzadeh H et al. Isolation, differentiation and characterization of mesenchymal stem cells from human bone marrow. Gastroenterology & Hepatology 2017; 10: 208-213.
26. Gimble JM, Guilak F. Adipose-derived adult stem cells: isolation, characterization, and differentiation potential. Cytotherapy 2003; 5: 362-369.
27. Schäffler A, Büchler C. Concise review: adipose tissue-derived stromal cells-basic and clinical implications for novel cell-based therapies. Stem Cells 2007; 25: 818-827.
28. Huang S, Fu R, Shyu W. Adipose-derived stem cells: Isolation, characterization, and differentiation potential. Cell Transplantation 2013; 22: 701-709.
29. Taha MF, Hedayati V. Isolation, identification and multipotential differentiation of mouse adipose tissue-derived stem cells. Tissue and Cell 2010; 42: 211-216.
30. Sung JH, Yang HM, Park JB, Choi GS, Joh JW et al. Isolation and characterization of mouse mesenchymal stem cells. Transplantation Proceedings 2008; 40: 2649-2654.
31. El Atat O, Antonios D, Hilal G, Hokayem N, Abou-Ghoch J et al. An evaluation of the stemness, paracrine, and tumorigenic characteristics of highly expanded, minimally passaged adipose-derived stem cells. PLoS One 2016; 11: e0162332.